# $Ca^{2+}$-dependent inactivation of the class C L-type $Ca^{2+}$ channel is a property of the $\alpha_1$ subunit

Xiangang Zong*, Franz Hofmann

*Institut für Pharmakologie und Toxikologie der Technischen Universität München, Biedersteiner Str. 29, 80802 München, Germany*

Received 20 November 1995; revised version received 30 November 1995

**Abstract The stably expressed $Ca^{2+}$ channel $\alpha_{1C\text{-}a}$ and $\alpha_{1C\text{-}b}$ subunit were used to investigate the molecular basis for $Ca^{2+}$-dependent inactivation of the L-type current. The $Ba^{2+}$ current ($I_{Ba}$) of both channels had similar kinetics and inactivated with one time constant of about 400 ms at +20 mV, whereas the $Ca^{2+}$ current ($I_{Ca}$) could be fitted only with a bi-exponential function. The fast ($\tau_f$) and the slow ($\tau_s$) time constant were about 20 ms and 400 ms, respectively. The inactivation of $I_{Ca}$ strongly depended on the entry of $Ca^{2+}$ as shown by prepulses and variation of the intracellular $Ca^{2+}$ chelator. Coexpression of the $\alpha_{1C}$ subunits with the auxiliary $\alpha_2/\delta$ and $\beta$ subunits accelerated the voltage-dependent but not the $Ca^{2+}$-dependent inactivation of the channels. These results suggest that the $\alpha_{1C}$ subunit of L-type $Ca^{2+}$ channels itself mediates the $Ca^{2+}$-dependent inactivation of the current.**

*Key words:* $Ca^{2+}$-dependent inactivation; L-type $Ca^{2+}$ channel; Intracellular $Ca^{2+}$ buffer; CHO cell; HEK 293 cell

## 1. Introduction

$Ca^{2+}$ entry through voltage-gated L-type $Ca^{2+}$ channels provides in many cells the intracellular $Ca^{2+}$ ($[Ca^{2+}]_i$) and triggers thereby many physiological functions such as contraction or neuro-secretion. The opening of these channels is tightly controlled to prevent overload of the cell with $Ca^{2+}$. These channels inactivate rapidly in response to depolarization and an increase in $[Ca^{2+}]_i$. This voltage- and $Ca^{2+}$-dependent inactivation is an important negative feedback mechanism to prevent $Ca^{2+}$ overload and cell death.

Despite its importance and the fact that $Ca^{2+}$-dependent inactivation of $Ca^{2+}$ channels [1] has been discovered nearly 20 years ago, the molecular basis of the $Ca^{2+}$-dependent inactivation remained controversial. Voltage-gated L-type $Ca^{2+}$ channels are heterotetramers consisting of three subunits, named $\alpha_1$, $\alpha_2/\delta$, and $\beta$. The $\alpha_1$ subunit forms the functional $Ca^{2+}$ conducting unit [2]. The $\alpha_2/\delta$ and $\beta$ subunits are auxiliary subunits which increase the current amplitude and affect the voltage-dependent activation and inactivation of $Ca^{2+}$ channels [3–6]. There is no agreement whether or not the $Ca^{2+}$-dependent inactivation requires the presence of auxiliary subunits in addition to the $\alpha_1$ subunit. Tanabe and coworkers [7,8] reported that $Ca^{2+}$-dependent inactivation required the coexpression of the $\alpha_1$ subunit with the other auxiliary subunits, especially that of the $\beta$ subunit. In contrast, other groups [9–12] observed $Ca^{2+}$-dependent inactivation of the expressed rabbit cardiac L-type $\alpha_{1C}$ subunit in the absence of the auxiliary subunits. To study the $Ca^{2+}$-dependent inactivation of L-type $\alpha_{1C}$ channels, we investigated the $Ca^{2+}$ ($I_{Ca}$) and $Ba^{2+}$ ($I_{Ba}$) currents of cardiac ($\alpha_{1C\text{-}a}$) and smooth muscle ($\alpha_{1C\text{-}b}$) subunits stably expressed in Chinese hamster ovary (CHO) and human embryonic kidney (HEK 293) cells in the absence and presence of the auxiliary subunits. Both channels showed $Ca^{2+}$-dependent inactivation in the absence of the expressed auxiliary subunits.

## 2. Materials and methods

### 2.1. Cell transfection and culture

CHO and HEK 293 cells were transfected stably with the coding region of the $\alpha_{1C\text{-}a}$ [13] and $\alpha_{1C\text{-}b}$ [14] subunit, respectively, as described in Zong et al. [15]. The HEK 293 cell line was used to express transiently the $\alpha_2/\delta$ and $\beta_2$ [16] subunit. The properties of the $\Delta$C1733 HEK 293 cell line have been described [17]. Media, sera and fetal calf serum were obtained from Gibco, Eggenstein. Cell culture was carried out by common standard procedures.

### 2.2. Electrophysiological recording

The patch pipettes with resistances 2 to 3 M$\Omega$ were filled with intracellular solution containing in mM: 102 CsCl, 10 tetraethylammonium chloride (TEA-Cl), 1.0 $MgCl_2$, 3.0 $Na_2$-ATP, 5.0 4-(2-hydroxyethyl)-l-piperazine-ethane-sulphonic acid (HEPES), 10 ethylene bis (oxonitrilo) tetraacetate (EGTA), pH 7.4 adjusted with CsOH. In some experiments, EGTA was replaced by 20 mM 1,2-bis(2-aminophenoxy) ethane-*N*,*N*,*N*′,*N*′-tetra acetic acid (BAPTA) and CsCl was reduced to 92 mM. The low chloride pipette solution contained in mM: 140 *N*-methyl-D-glucamine, 2.0 $MgCl_2$, 3.0 $Na_2$-ATP, 5.0 HEPES, 10 EGTA, pH 7.4 adjusted with methanesulphonic acid. A double-barrelled pipette placed 200 $\mu$m away from the cell was used to switch the superfusion from bath solution containing $Ca^{2+}$ ($Ca^{2+}$ Tyrode's solution) to that containing $Ba^{2+}$ ($Ba^{2+}$ Tyrode's solution). $Ca^{2+}$ or $Ba^{2+}$ Tyrode's solution contained in mM: 82 NaCl, 10 $CaCl_2$ or $BaCl_2$, 5.0 CsCl, 30 TEA-Cl, 1.0 $MgCl_2$, 10 HEPES, 5.0 glucose, pH 7.4 adjusted with NaOH. The chloride free bath solution contained in mM: 100 TEA-OH, 10 $Ca(OH)_2$ or $Ba(OH)_2$, 5.0 4-aminopyridine, 10 HEPES, 10 glucose, pH 7.4 adjusted with methanesulphonic acid.

Whole cell currents were recorded using a List EPC 7 amplifer and pCLAMP software (Axon Instruments) running on a IBM compatible computer. Data were digitized at 10 kHz, filtered at 2 kHz and analysed with AUTESP. Capacitative transients and leak currents were subtracted using linearly scaled currents elicited by a step from −80 to −90 mV. All experiments were done at room temperature (20°C–23°C). If not stated otherwise, the holding potential (HP) was −80 mV and test pulses were to +20 mV for 500 ms at 0.1 Hz. The average of the current measured between 10 and 15 ms after the depolarization step was taken as individual peak current. The inactivation trace of individual currents was fitted using a mono-exponential function: $I(t) = a + b^{(-t/\tau)}$, or a bi-exponential function: $I(t) = a + b^{(-t/\tau_f)} + c^{(-t/\tau_s)}$, where $I(t)$ is the inactivating current as a function of time, $a$ is the current amplitude at $t = \infty$, $b$ and $c$ are the amplitudes of the time-dependent components, $\tau_f$ and $\tau_s$ are the fast and slow time constant of inactivation, respectively. The parameters in the equations were determined by a least-squares fitting routine described by Marquardt [18]. All values are given as mean ± S.E.M.

*Corresponding author. Fax: (49) (89) 38493261.


*SSDI* 0014-5793(95)01434-9

## 3. Results and discussion

### 3.1. The stably expressed $\alpha_{1C}$ subunit channel inactivates in a $Ca^{2+}$-dependent manner

The $\alpha_{1C\text{-}a}$ subunit channel was stably expressed in CHO cells. As shown in Fig. 1, the peak current amplitude of the $\alpha_{1C\text{-}a}$ channel was reduced to less than one fourth if the charge carrier was changed from $Ba^{2+}$ to $Ca^{2+}$ (21.7 ± 3.4%; $n = 3$). This reduction in amplitude is probably the result of a smaller conductance for $Ca^{2+}$ than $Ba^{2+}$ [19]. The $I$–$V$ curve for $I_{Ca}$ was shifted by 10 to 20 mV to positive potentials compared with that of $I_{Ba}$ (Fig. 1C). Most likely this shift was caused by the difference in surface potential [20]. The corresponding inactivation

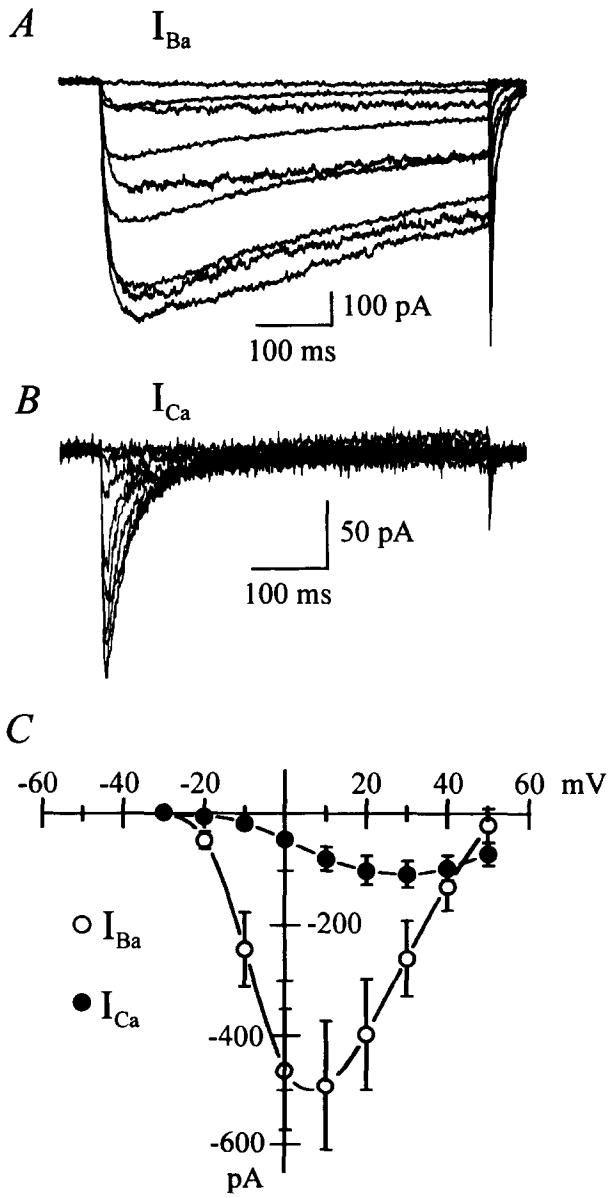


Fig. 1. $I_{Ba}$ and $I_{Ca}$ of the $\alpha_{1C\text{-}a}$ subunit inactivate differently. The $\alpha_{1C\text{-}a}$ subunit was expressed stably in a CHO cell. The traces of $I_{Ba}$ (A) and $I_{Ca}$ (B) were evoked by depolarizing steps from a holding potential of −80 mV to −30 to +50 mV in 10 mV increments. Both currents were measured in the presence of 1 μM Bay K 8644 because $I_{Ca}$ was to small to yield reliable fits for the inactivation traces. C: The $I$–$V$ relation of $I_{Ba}$ (○) and $I_{Ca}$ (●) ($n = 3$ cells).

traces of $I_{Ba}$ could be fitted very well by a mono-exponential function with a time constant ($\tau_i$) of 404 ± 26.7 ms ($n = 3$) at +20 mV. In contrast, the inactivating traces of $I_{Ca}$ could be fitted only by a bi-exponential function with a fast ($\tau_f$) and a slow ($\tau_s$) time constant at all potentials between −20 and +50 mV. The $\tau_f$ and $\tau_s$ at +20 mV were 18.3 ± 2.8 ms ($n = 3$) and 396 ± 18.3 ms ($n = 3$), respectively. The time constants $\tau_f$ and $\tau_s$ may represent $Ca^{2+}$- and voltage-dependent inactivation of $I_{Ca}$, respectively, whereas $I_{Ba}$ appeared to inactivate only by a voltage-dependent mechanism.

To test the generality of these results, similar experiments were carried out with the stably expressed $\alpha_{1C\text{-}b}$ subunit. This cell line had higher $I_{Ca}$ densities which allowed a detailed analysis of the inactivation kinetics in the absence of the $Ca^{2+}$ channel agonist Bay K 8644. Fig. 2 shows the voltage- and $Ca^{2+}$-dependent inactivation of $\alpha_{1C\text{-}b}$ channels stably expressed in HEK 293 cells. Like the $\alpha_{1C\text{-}a}$ channel, the $I_{Ca}$ and $I_{Ba}$ of the $\alpha_{1C\text{-}b}$ channel inactivated with a bi- and a mono-exponential function, respectively (Fig. 2A). The time constant of $I_{Ba}$ inactivation was almost identical to the slow time constant of $I_{Ca}$ inactivation and had similar voltage-dependence (Fig. 2B). The $I_{Ca}$ inactivated additionally with a fast phase (Fig. 2A,C). The voltage-dependence of the $\tau_f$ of $I_{Ca}$ can be explained by a voltage-dependent $Ca^{2+}$ entry through the L-type $Ca^{2+}$ channels [21]. These experiments suggested that the $\alpha_{1C\text{-}b}$ channel like the $\alpha_{1C\text{-}a}$ channel possesses the property of $Ca^{2+}$-dependent inactivation.

### 3.2. $Ca^{2+}$-dependent inactivation depends on $Ca^{2+}$ entry

In order to determine the $[Ca^{2+}]_i$ dependence of the inactivation of the $\alpha_{1C\text{-}b}$ channel, a double pulse protocol was used in which the effect of a prepulse and the intracellular $Ca^{2+}$ buffer on $I_{Ba}$ and $I_{Ca}$ of the following test pulse was investigated (Fig. 3). A 50 ms prepulse, which is to short to induce steady state inactivation of the channel, should decrease the magnitude of $I_{Ca}$ during the following test pulse, since $[Ca^{2+}]_i$ increases during the prepulse. The same prepulse should not affect the size of $I_{Ba}$ during the test pulse. The experiments shown in Fig. 3 support this prediction, i.e. a prepulse to +20 mV, a membrane potential at which $I_{Ca}$ of the prepulse is activated maximally (Fig. 3A), inactivated $I_{Ca}$ of the test pulse by more than 60% (Fig. 3B). The prepulse to +20 mV, however, had only a small effect on $I_{Ba}$ of the test pulse. As predicted, the $I$–$V$ relation of the prepulse current ($I_{pp}$) was inversely correlated with that of the test pulse current ($I_{tp}$), if $Ca^{2+}$ was used as charge carrier, i.e. the $I_{pp}$ at +20 mV prepulse was maximal but the $I_{tp}$ at same prepulse was minimal (Fig. 3B). This inverse relation is a strong argument [21] that $Ca^{2+}$ entry induced inactivation of the $\alpha_{1C}$ channel. In contrast, the $I_{tp}$ of $I_{Ba}$ inactivated maximally by 22% even if the prepulse was positive to +40 mV supporting the prediction that the short prepulses did not induce significant voltage-dependent steady state inactivation of the channel (see below).

The $[Ca^{2+}]_i$-dependent inactivation of the channel should be reduced by dialysing the cell with BAPTA, a faster $Ca^{2+}$ chelator than EGTA. The increase in the intracellular $Ca^{2+}$-buffer concentration from 10 mM EGTA to 20 mM BAPTA had only a slight effect on the $I$–$V$ relations of $I_{Ca}$ and $I_{Ba}$ (Fig. 3C), but reduced remarkably the decrease in $I_{Ca}$ amplitude induced by $Ca^{2+}$ entry (Fig. 3D). The inactivation of $I_{Ca}$ was still more pronounced than that of $I_{Ba}$ (Fig. 3D). Interestingly, the

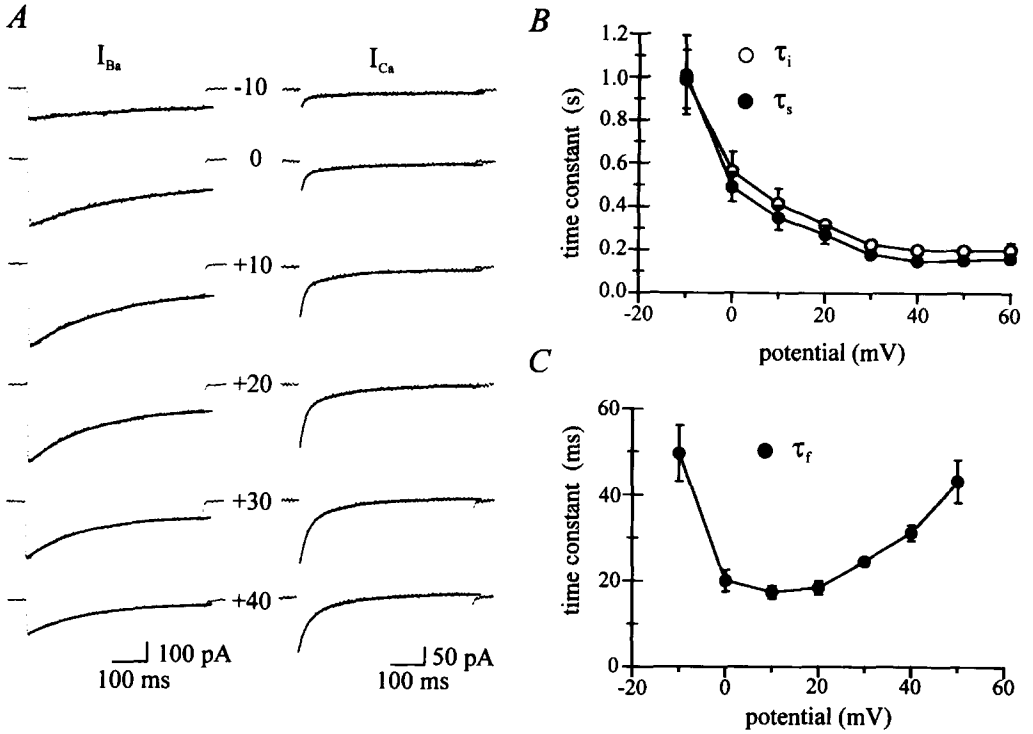


Fig. 2. Voltage- and $Ca^{2+}$-dependent inactivation the of $\alpha_{1C\text{-}b}$ subunit stably expressed in a HEK 293 cell. (A) The traces of $I_{Ba}$ (left pannel) and $I_{Ca}$ (right pannel) were elicited by depolarizing steps from a holding potential of −80 mV to the potentials indicated. The continuous lines show the fits with mono-($I_{Ba}$) and bi-exponential ($I_{Ca}$) functions. (B,C) Voltage-dependence of the inactivation of $I_{Ba}$ and $I_{Ca}$. $\tau_i$: time constant of $I_{Ba}$ inactivation. $\tau_s$ and $\tau_f$: slow and fast time constant of $I_{Ca}$ inactivation ($n = 6$).

decrease in $I_{Ba}$ amplitude induced by prepulses positive to +20 mV was also markedly reduced by 20 mM BAPTA (Fig. 3D) suggesting that the decrease in $I_{Ba}$ observed in the presence of 10 mM EGTA (Fig. 3B) was caused by a $Ca^{2+}$ contamination of the $Ba^{2+}$-Tyrode's solution. The experiments of Fig. 3D indicated further that the increase in the intracellular $Ca^{2+}$ buffering capacity prevented only partially the $Ca^{2+}$-dependent inactivation of the channel in agreement with the idea that the

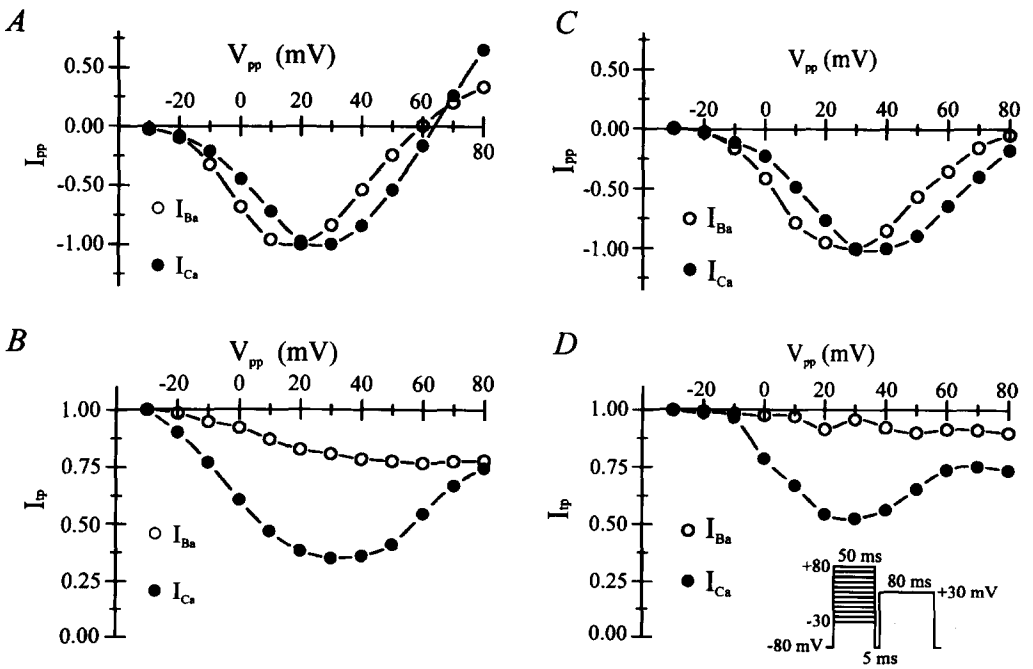


Fig. 3. $I_{Ca}$ inactivation depends on $Ca^{2+}$ entry through the $\alpha_{1C\text{-}b}$ channel. Relations between the currents (○, $I_{Ba}$; ●, $I_{Ca}$) and prepulse potential ($V_{pp}$) in the cells dialysed with the pipette solution containing 10 mM EGTA (A and B) or 20 mM BAPTA (C and D). $I_{pp}$ and $I_{tp}$ were the currents elicited by the pre- and test pulse, respectively. The currents were normalized to the maximal current induced by the prepulse in A and C and to the current induced by a test pulse without prepulse in B and D. The inset in D shows the double pulse protocol.

increase of the local $Ca^{2+}$ concentration near or within the channel pore is more important for the $Ca^{2+}$-dependent inactivation of L-type $Ca^{2+}$ channels than the increase of total $[Ca^{2+}]_i$.

A potential pitfall of the above experiments could be the presence of outward chloride currents in these cells since they could mask the inactivation of $I_{Ca}$. To exlude this possibility, a chloride free bath solution and a low chloride pipette solution (4 mM chloride) was used. Under these conditions, the reversal potential of $I_{Ba}$ and $I_{Ca}$ was shifted to more positive membrane potentials without affecting significantly the membrane potentials inducing activation and maximal inward current (Fig. 4A,B). The inactivating kinetics of $I_{Ba}$ and $I_{Ca}$ were not changed by the chloride free solutions (Fig. 4C) supporting the notion that $Ca^{2+}$-dependent inactivation of the $\alpha_{1C}$ channels was not obscured by a chloride conductance which may be present in HEK 293 cells.

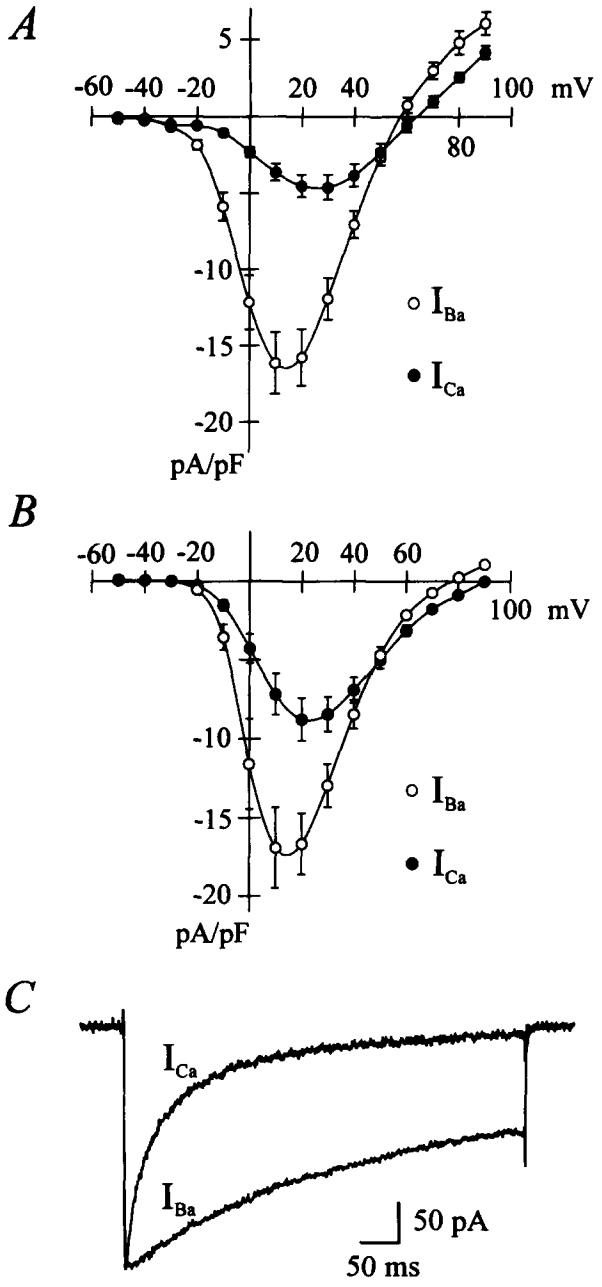


Fig. 4. $Ca^{2+}$-dependent inactivation of the $\alpha_{1C\text{-}b}$ channel is not masked by chloride currents. (A,B) $I$–$V$ curves of $I_{Ba}$ (○) and $I_{Ca}$ (●) recorded in cells perfused with the chloride containing (A, $n = 6$) and chloride free (B, $n = 7$) bath and pipette solution. (C) $I_{Ba}$ and $I_{Ca}$ traces recorded in the cell perfused with the chloride free solutions depolarised to +20 mV. The $I_{Ca}$ was normalized with a factor of 2.2. The continuous lines show the fits: $\tau_i$, 281ms; $\tau_f$, 22.2 ms and $\tau_s$, 220 ms.

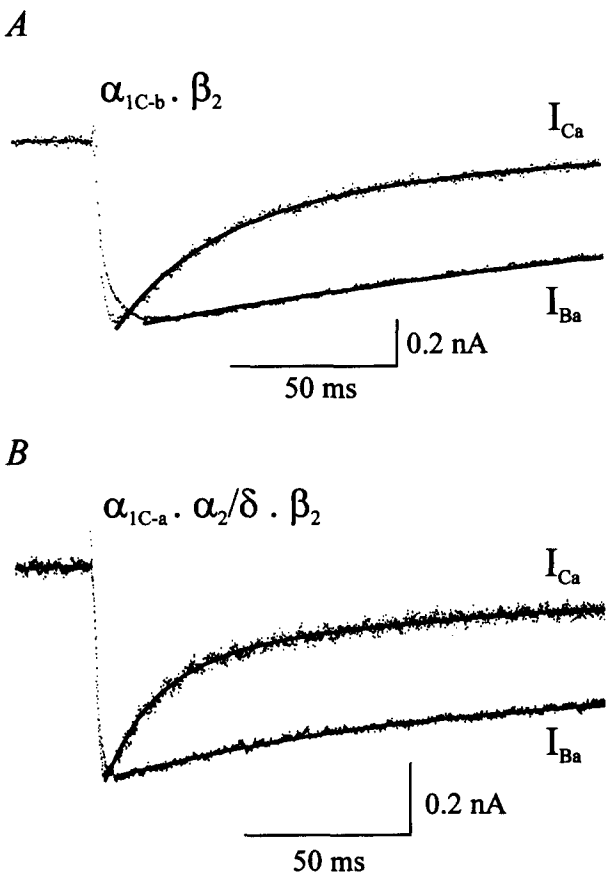


Fig. 5. $Ca^{2+}$-dependent inactivation does not require auxiliary subunits. A: Current traces recorded in the HEK 293 cell stably expressing the $\alpha_{1C\text{-}b}$ subunit and transiently transfected with the $\beta_{2a}$ subunit. $I_{Ba}$ was evoked at +20 mV. $\tau_i$ was 228 ms. $I_{Ca}$ was evoked by a pulse to +20 mV and normalized with a factor of 3.3. $\tau_f$ and $\tau_s$ were 23.2 ms and 239 ms, respectively. The continuous lines show the fits. (B) $I_{Ba}$ and $I_{Ca}$ recorded in the HEK 293 cell transfected transiently with the $\alpha_{1C\text{-}a}$, $\alpha_2/\delta$ and $\beta_{2b}$ subunit. $I_{Ca}$ was normalized with a factor of 2.5. $\tau_i$: 212 ms; $\tau_f$: 21.5 ms; $\tau_s$: 223 ms.

### 3.3. $Ca^{2+}$-dependent inactivation does not require auxiliary subunits

As previously described [3,4,15,22], the coexpression of the $\alpha_2/\delta$ and $\beta_2$ subunit with the $\alpha_{1C}$ subunit increased the current density and the inactivation of the channels. Fig. 5 illustrates with two examples that the auxiliary subunits did not affect grossly $I_{Ca}$ and $I_{Ba}$ traces of the two $\alpha_{1C}$ channels. The fast inactivation time constant $\tau_f$ of $I_{Ca}$ was not changed by the auxiliary subunits. In contrast, the voltage-dependent inactivation time constants ($\tau_i$ and $\tau_s$) were accelerated (Tab. 1). The fact that the auxiliary subunits had no effect on $\tau_f$ supports strongly the notion that they are not required for $Ca^{2+}$-dependent inactivation of the channel.

The results of this paper clearly show that the $\alpha_{1C}$ subunit of

Table 1
Summary of inactivation time constants

| Channel composition | $n$ | $I_{Ba}$ $\tau_i$ (ms) | $I_{Ca}$ | | $I_{Ca}/I_{Ba}$ (%) |
|---|---|---|---|---|---|
| | | | $\tau_f$ (ms) | $\tau_s$ (ms) | |
| $\alpha_{1C-a}$ | 3 | 404 ± 26.7 | 18.3 ± 2.8 | 396 ± 18.3 | 21.7 |
| $\alpha_{1C-b}$ | 6 | 317 ± 23.3 | 18.4 ± 1.6 | 272 ± 41.9 | 28.6 |
| $\alpha_{1C-b}\cdot\beta_{2a}$ | 4 | 213 ± 55.4 | 19.2 ± 2.8 | 154 ± 30.9 | 34.0 |
| $\alpha_{1C-a}\cdot\alpha_2/\delta\cdot\beta_{2b}$ | 5 | 186 ± 25.6 | 15.7 ± 2.2 | 160 ± 11.2 | 37.1 |
| $\Delta$C1733 | 5 | 333 ± 29.8 | 18.5 ± 2.31 | 285 ± 66.6 | 31.7 |

The $\alpha_{1C-a}$ and $\alpha_{1C-b}$ channels were stably expressed in CHO and HEK 293 cells, respectively. The other subunits were transiently expressed in HEK 293 cells. The currents were elicited by pulses from a holding potential of −80 mV to +20 mV. The values are given in mean ± S.E.M. For further details see text and legends to figures.

the L-type $Ca^{2+}$ channel possesses the $Ca^{2+}$-dependent inactivation property. This signifies that the $\alpha_{1C}$ subunit not only has a pore which selects for $Ca^{2+}$ but has also a $Ca^{2+}$ binding site that is responsible for $Ca^{2+}$-dependent inactivation [23]. The latter site has not been identified. The $Ca^{2+}$ binding site must be located very close to the inner mouth of the channel pore because (a) even the strong intracellular $Ca^{2+}$ buffering by 20 mM BAPTA failed to abolish completely $Ca^{2+}$-dependent inactivation and (b) the $\Delta$C1733 $\alpha_{1C}$ subunit, which was truncated at amino acid 1733 and lacked the last 438 amino acids of the carboxy-terminus [17,24] showed also $[Ca^{2+}]_i$-dependent inactivation (Table 1). It has been suggested that the $\alpha_{1C}$ subunit containes an EF-hand domain located almost directly after the last transmembrane segment IVS6 [25]. It is possible that this structure which is close to the innner mouth of the channel pore mediates $Ca^{2+}$-dependent inactivation of L-type $Ca^{2+}$ channels [12].

*Acknowledgements*: This work was supported in part by grants from Deutsche Forschungsgemeinschaft, Fond der Chemischen Industrie and SET.

## References

[1] Brehm, P. and Eckert, R. (1978) Science 202, 1203–1206.
[2] Hofmann, F., Biel, M. and Flockerzi, V. (1994) Annu. Rev. Neurosci. 17, 399–418.
[3] Singer, D., Biel, M., Lotan, I., Flockerzi, V., Hofmann, F. and Dascal, N. (1991) Science 253, 1553–1557.
[4] Wei, X.Y., Perez-Reyes, E., Lacerda, A.E., Schuster, G., Brown, A.M. and Birnbaumer, L. (1991) J. Biol. Chem. 266, 21943–21947.
[5] Neely, A., Wei, X., Olcese, R., Birnbaumer, L. and Stefani, E. (1993) Science 262, 575–578.
[6] Olcese, R., Qin, N., Schneider, T., Neely, A., Wei, X.Y., Stefani, E. and Birnbaumer, L. (1994) Neuron 13, 1433–1438.
[7] Tanabe, T., Beam, K.G., Adams, A., Niidome, T. and Numa, S. (1990) Nature 346, 567–569.
[8] Zong, S., Zhou, J. and Tanabe, T. (1994) Biochem. Biophys. Res. Commun. 201, 1117–1123.
[9] Welling, A., Kwan, Y.W., Bosse, E., Flockerzi, V., Hofmann, F. and Kass, R.S. (1993) Circ. Res. 73, 974–980.
[10] Mehrke, G., Zong, X, G., Flockerzi, V. and Hofmann, F. (1994) J. Pharmacol. Exp. Ther. 271, 1483–1488.
[11] Neely, A., Olcese, R., Wei, X., Birnbaumer, L. and Stefani, E. (1994) Biophys. J. 66, 1895–1903.
[12] de Leon, M., Jones, L., Perez-Reyes, E., Wei, X., Soong, T.W., Snutch, T.P. and Yue, D.T. (1995) Biophys. J. 68, A13.
[13] Mikami, A., Imoto, K., Tanabe, T., Niidome, T., Mori, Y., Takeshima, H., Narumiya, S. and Numa, S. (1989) Nature 340, 230–233.
[14] Biel, M., Ruth, P., Bosse, E., Hullin, R., Stühmer,W., Flockerzi, V. and Hofmann, F. (1990) FEBS Lett. 269, 409–412.
[15] Zong X.G., Schreieck, J., Mehrke, G., Welling, A., Schuster, A., Bosse, E., Flockerzi, V. and Hofmann, F. (1995) Pflügers Arch. 430, 340–347.
[16] Hullin, R., Singer-Lahat, D., Freichel, M., Biel, M., Dascal, N., Hofmann, F. and Flockerzi, V. (1992) EMBO J. 11, 885–890.
[17] Seisenberg, C., Welling, A., Schuster, A. and Hofmann, F. (1995) Naunyn-Schmiedeberg's Arch. Pharmacol. 352, in press.
[18] Marquardt, D.W. (1963) J. Society for Industrial and Applied Mathematics 11, 431–441.
[19] Yue, D.T. and Marban, E. (1990) J. Gen. Physiol. 95, 911–939.
[20] McDonald, T.F., Pelzer, S., Trautwein, W. and Pelzer, D.J. (1994) Physiol. Rev. 74, 365–507.
[21] Hille, B. (1992) Ionic Channels in Excitable Membranes 2nd ed., Sinauer Associates, Sunderland, MA.
[22] Welling, A., Bosse, E., Cavalié, A., Bottlender, R., Ludwig, A., Nastainczyk, W., Flockerzi, V. and Hofmann, F. (1993) J. Physiol. (Lond) 471, 749–765.
[23] Imredy, J.P. and Yue, D.T. (1994) Neuron 12, 1301–1318.
[24] Wei, X.Y., Neely, A., Lacerda, A.E., Olcese, R., Stefani, E., Perez-Reyes, E. and Birnbaumer, L. (1994) J. Biol. Chem. 269, 1635–1640.
[25] Babitch, J. (1990) Nature 346, 321–322.